



Transient energy growth for the Lamb–Oseen vortex

Arnaud Antkowiak, Pierre Brancher

► To cite this version:

Arnaud Antkowiak, Pierre Brancher. Transient energy growth for the Lamb–Oseen vortex. *Physics of Fluids*, 2004, 16 (1), pp.L1-L4. 10.1063/1.1626123 . hal-00086131

HAL Id: hal-00086131

<https://hal.science/hal-00086131>

Submitted on 18 Jul 2006

HAL is a multi-disciplinary open access archive for the deposit and dissemination of scientific research documents, whether they are published or not. The documents may come from teaching and research institutions in France or abroad, or from public or private research centers.

L'archive ouverte pluridisciplinaire **HAL**, est destinée au dépôt et à la diffusion de documents scientifiques de niveau recherche, publiés ou non, émanant des établissements d'enseignement et de recherche français ou étrangers, des laboratoires publics ou privés.

Transient energy growth for the Lamb-Oseen vortex

Arnaud Antkowiak¹ and Pierre Brancher¹

¹*Institut de Mécanique des Fluides de Toulouse,*

Allée du Professeur Camille Soula, 31400 Toulouse, France

(Dated: September 12, 2003)

The transient evolution of infinitesimal flow disturbances which optimally induce algebraic growth in the Lamb-Oseen (gaussian) vortex is studied using a direct-adjoint technique. This optimal perturbation analysis reveals that the Lamb-Oseen vortex allows for intense amplification of kinetic energy for 2D and 3D perturbations of azimuthal wavenumber $m = 1$. In both cases, the disturbances experiencing the most growth initially take the form of concentrated spirals at the outer periphery of the vortex which rapidly excite bending waves within the vortex core. In the limit of large wavelengths, the optimal perturbation leads to arbitrarily large growths via an original scenario combining the Orr mechanism with vortex induction.

PACS numbers: 47.32.-y, 47.32.Cc, 47.20.-k, 47.20.Pc, 02.30.Yy, 02.60.Pn, 02.70.Hm, 02.70.Jn

The stability properties of vortices have received considerable attention in recent years partly because of a renewed interest in the dynamics of trailing vortices behind aircrafts. More specifically, the strong and persistent counter-rotating vortex pair generated at the trailing edge of airplane wings represent a potential hazard to forthcoming planes thus limiting take-off and landing cadences in airports. It has been shown in the last decades that these vortices are unstable to long-¹ and short-wave² instabilities due to the underlying

strain field induced by the companion vortex. Moreover the presence of an axial flow is at the origin of other instability mechanisms³.

By contrast, an isolated vortex with no axial flow and monotonically decreasing positive vorticity, hereafter called an axisymmetric monopole, is linearly stable with respect to 2D and 3D perturbations (see for instance the temporal stability analysis of Fabre⁴). In particular it is stable with regard to both the centrifugal and inflexion-point Rayleigh criteria. Stability analyses of this kind of vortex generally focus on 2D perturbations. In the inviscid case, a deformed vortex relaxes toward an axisymmetric state after an exponential (Landau) damping followed by algebraic decay at long times of the initial asymmetric perturbations^{5,6}. At large but finite Reynolds numbers, asymmetric perturbations asymptotically decay on a $\text{Re}^{1/3}$ time scale via a shear/diffusion mechanism^{7,8}.

Interesting algebraic evolution of 2D disturbances has also been reported in the case of inviscid hollow hurricane-like vortices^{9,10}: long time asymptotics has revealed the possibility for linear growth of the perturbation kinetic energy even if the flow is exponentially stable. But this mechanism is only active under the necessary condition that the basic flow angular velocity has a local maximum other than at the vortex axis, which is not the case for the axisymmetric monopole. Yet a generalized stability analysis of monopolar vortices maintained by radial inflow has also revealed transient growth for 2D spiral-shaped perturbations¹¹. Moreover the same authors have found that the linear response of these flows to random forcing involved a similar spiral-shaped dominant structure¹². Finally recent theoretical studies¹³ have suggested that interactions between a vortex and 3D external turbulence could excite bending waves, via a dominant linear process that may eventually destroy the vortex after about 10 rotation times in the non-linear regime.

In that context our objective in this letter is to present preliminary results revealing

the potential for intense transient amplification of kinetic energy for specific perturbations (*optimal perturbation*) in the linear regime. It is argued that this transient growth could eventually trigger a nonlinear transition in an otherwise linearly stable vortex.

The present work analyzes the temporal evolution of infinitesimal 3D perturbations with velocity components in cylindrical co-ordinates $\mathbf{u}(r, \theta, z, t) = (u_r, u_\theta, u_z)^T$ in a steady incompressible axisymmetric vortex flow $\mathbf{U}(r) = (0, r\Omega, 0)^T$. The basic flow under consideration here is the Lamb-Oseen model, with angular velocity $\Omega(r) = [1 - \exp(-r^2)]/r^2$ and associated axial vorticity $Z(r) = 2\exp(-r^2)$. Here space and time have been respectively non-dimensionalized by the vortex radius r_0 and the (maximum) angular velocity at the axis Ω_0 . The Reynolds number based on these characteristic scales is $\text{Re} = \Omega_0 r_0^2 / \nu$, where ν denotes the kinematic viscosity. Linearizing the Navier-Stokes equations around this basic flow, it is possible to eliminate the perturbation pressure and axial velocity to get a complete description of the perturbation in terms of $\tilde{\mathbf{v}} = (u_r, u_\theta)^T$. Then, injecting a classical normal modes decomposition $\tilde{\mathbf{v}}(r, \theta, z, t) = \mathbf{v}(r, t) \exp[i(kz + m\theta)]$, where k (real) and m (integer) are respectively the axial and azimuthal wavenumbers, yields the following system for \mathbf{v} , rewritten in compact form:

$$\mathbf{F}(\mathbf{v}) = \mathbf{L} \frac{\partial \mathbf{v}}{\partial t} + \mathbf{C} \mathbf{v} - \frac{1}{\text{Re}} \mathbf{D} \mathbf{v} = \mathbf{0}, \quad (1)$$

with the associated boundary conditions that the perturbation is regular at $r = 0$ and tends to 0 at infinity. Derivation of (1) is straightforward⁴. \mathbf{D} is a viscous diffusion operator and the operator \mathbf{L} results from the elimination of pressure and axial velocity from the original linearized Navier-Stokes equations. Disturbance and basic flow are coupled through the advection operator \mathbf{C} .

Classical linear stability theory focuses on the long time behaviour of the normal modes by assuming exponential time dependence of the form $\mathbf{v}(r, t) = \mathbf{v}(r) e^{-i\omega t}$. The analysis

then reduces to an eigenvalue problem for the complex pulsations ω , which are all stable for the Lamb-Oseen vortex⁴. Nevertheless it is noteworthy that the advection operator \mathbf{C} is highly non-normal, except in the trivial case $k = m = 0$ or in the special case of solid-body rotation. This property, here due to differential rotation, implies that short time transient amplification can be anticipated¹⁴.

This conjecture can be addressed by computing the optimal perturbation, *i.e.* the initial condition which maximizes the energy gain $G(\tau) = E_\tau/E_0$ during a finite time interval $[0, \tau]$, where the perturbation energy at time t is given by

$$E_t = \int_0^\infty (\bar{u}_r u_r + \bar{u}_\theta u_\theta + \bar{u}_z u_z) r \, dr \Big|_t$$

Here the overbars indicate transpose conjugate quantities.

Different techniques can be used to determine the optimal initial conditions^{15–18}. The formalism employed in the present work comes from optimal control theory. It has been successfully used to compute the optimal perturbation in swept boundary layers¹⁹. Since we follow closely the protocol described in Corbett and Bottaro¹⁹, we only give a synthetic presentation of this approach in the following.

The optimization problem lies in maximizing the energy growth $G(\tau)$ (the *objective*) at a given time τ under the *constraints* of respecting (1) and the associated boundary conditions. The initial condition \mathbf{v}_0 is used as a *control* to be adjusted in order to meet the objective. This constrained optimization problem can be solved by considering the equivalent unconstrained problem for the Lagrangian functional

$$\mathcal{L}(\mathbf{v}, \mathbf{v}_0, \mathbf{a}, \mathbf{c}) = G(\tau) - \langle \mathbf{F}(\mathbf{v}), \mathbf{a} \rangle - \langle \mathbf{H}(\mathbf{v}, \mathbf{v}_0), \mathbf{c} \rangle,$$

introducing the adjoint variables $\mathbf{a}(r, t) = (a, b)^T$ and $\mathbf{c}(r) = (c, d)^T$ which play the role of Lagrange multipliers. Here $\mathbf{H}(\mathbf{v}, \mathbf{v}_0) = \mathbf{v}(r, 0) - \mathbf{v}_0(r)$ corresponds to the constraint that

the initial condition $\mathbf{v}(r, 0)$ matches the control $\mathbf{v}_0(r)$. The inner products appearing in the functional are

$$(\mathbf{p}, \mathbf{q}) = \int_0^\infty \bar{\mathbf{p}} \cdot \mathbf{q} \, r \, dr + \text{complex conjugate},$$

$$\langle \mathbf{p}, \mathbf{q} \rangle = \int_0^\tau (\mathbf{p}, \mathbf{q}) \, dt.$$

The task is then to determine \mathbf{v} , \mathbf{v}_0 , \mathbf{a} and \mathbf{c} which render \mathcal{L} stationary, *i.e.* corresponding to a local extremum. Setting to zero variations of \mathcal{L} with respect to these variables yields boundary conditions and the following (adjoint) system for the variable \mathbf{a}

$$\mathbf{F}^+(\mathbf{a}) = -\mathbf{L} \frac{\partial \mathbf{a}}{\partial t} + \mathbf{C}^+ \mathbf{a} - \frac{1}{\text{Re}} \mathbf{D} \mathbf{a} = \mathbf{0}, \quad (2)$$

where \mathbf{C}^+ is the adjoint operator of \mathbf{C} . It also yields transfer relations between the direct and adjoint variables at times $t = 0$ and $t = \tau$ as well as the expression of the optimal perturbation. The reader is referred to the paper by Corbett and Bottaro¹⁹ for the details of the derivation. The computation of the optimal perturbation is carried out via the following iterative algorithm: from an initial guess (random noise) \mathbf{v}_0 the direct system (1) is integrated to $t = \tau$; transfer relations are then applied to provide initial conditions for the backward-in-time integration of the adjoint system (2) until $t = 0$ thus providing improved initial conditions for the next iteration. In practice this procedure converges within 4 to 6 iterations (*i.e.* $G(\tau)$ varies less than 10^{-2}).

The spatial treatment of the direct and adjoint systems is based on a pseudospectral Chebyshev method²⁰. The equations are discretized on the Gauss-Lobatto grid algebraically mapped on the semi-infinite physical domain²⁰. All computations are done using MATLAB and the DMSuite package developed by Weideman and Reddy²¹. A special trick of the method has been to take advantage of the variables parity thus allowing to reduce the number of collocation points for a given accuracy⁴. Convergence tests have been performed

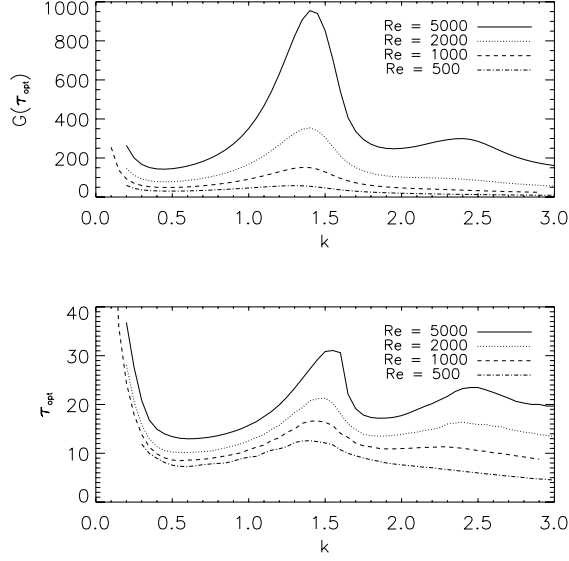


FIG. 1: Optimal energy growth and corresponding optimal time (in rotation periods) versus axial wavenumber.

by varying the stretching of the mapping and the number of collocation points from 40 to 120 without any dramatic changes in the results.

We next discuss preliminary results obtained for the particular case $m = 1$. The evolution of the optimal growth with respect to the axial wavenumber k is reported in figure 1, together with the corresponding time τ_{opt} at which it occurs. It can be seen that considerable growth can be reached, even at moderate Reynolds numbers. A remarkable feature is the presence of a relative maximum in energy near $k \simeq 1.4$ independently of the Reynolds number, indicating some three dimensional core sized mechanism efficient in redirecting energy from the mean flow to the perturbation. The energy value at this peak scales with the Reynolds number. Figure 2 shows the optimal disturbance structure corresponding to this maximum. This perturbation is at $t = 0$ composed of a set of spiraling vorticity sheets with a left-handed orientation that evolve so as to produce a strong bending wave within the vortex core. Due to three-dimensionality, the dynamics of such a perturbation is quite intricate (stretching

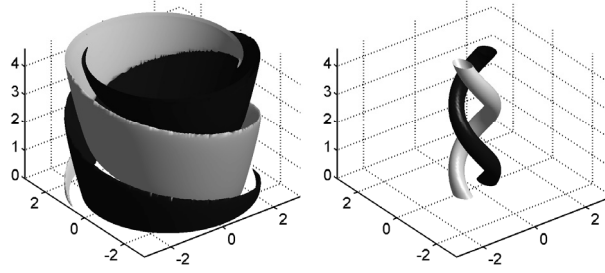


FIG. 2: Isosurfaces of axial vorticity for the optimal 3D case. The levels correspond to $\pm 80\%$ of maximum vorticity, at initial time (left) and optimal time (right).

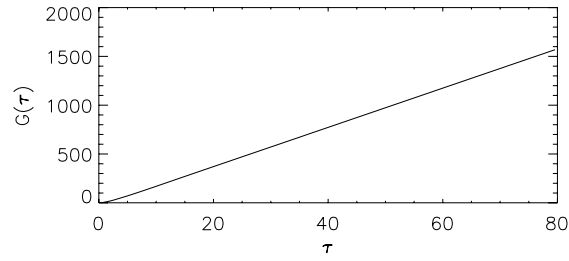


FIG. 3: Evolution of growth with terminal time (in rotation periods) in the 2D case at $\text{Re} = 1000$.

and tilting) and is not yet fully understood. Nevertheless, this dynamics might involve an analogue of the 3D mechanism analyzed by Farrell and Ioannou²². These authors present a generalization of the so-called Orr and lift-up mechanisms in plane shear flows which could constitute an interesting basis for the detailed analysis of the present results.

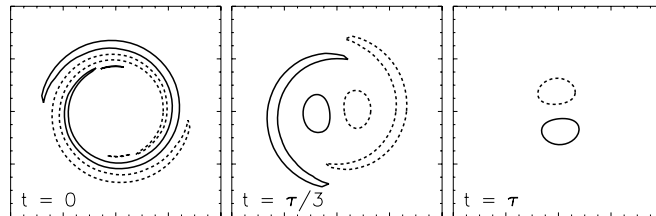


FIG. 4: Cross section of axial vorticity in the 2D case. The contour plot levels are $\pm 60\%$ of maximum absolute vorticity.

Though stretching and tilting vanish as large wavelengths are approached, the potential for substantial transient growth still exists. More specifically, the 2D limit exhibits a striking feature: the growth increases linearly²⁴ with terminal time τ (figure 3). Figure 4 depicts the evolution of a typical 2D optimal perturbation. The associated vorticity field initially takes the form of spirals that tend to thicken and to lie further from the vortex core as τ is increased (data not shown). This field satisfies the linearized vorticity equation:

$$\underbrace{\frac{\partial \omega}{\partial t} + \Omega \frac{\partial \omega}{\partial \theta}}_{\text{advection}} + \underbrace{u_r \frac{dZ}{dr}}_{\text{induction}} = \underbrace{\frac{1}{\text{Re}} \Delta \omega}_{\text{diffusion}}, \quad (3)$$

where three parts have been underbraced: an advection part which materially advects the vorticity perturbation, an induction part corresponding to redirection of vorticity from the mean flow to the disturbance (both parts coming from the linearization of the advection term in the complete equation) and a diffusion term. Let's examine how these terms interact as time evolves. The initial structure of the optimal perturbation is a set of vorticity sheets in the form of *leading* spirals (by opposition to *trailing* spirals, as for the advection of a passive scalar spot). This initial condition is located at the limb of the vortex, where the induction term is negligible. As time flows (middle of figure 4), the initial leading spirals are advected and unfolded via an analogue of the Orr mechanism. This process results in a local reorganization of the external perturbation vorticity that promotes vortex induction on the vortex axis as the spirals unroll. This original global sequel of the Orr mechanism initiated at the outer periphery of the vortex thus eventually leads to a contamination of the vortex core by exciting translational (bending) modes: quickly, an inner bipolar vortical structure grows, and at larger times most of the kinetic energy is associated with this 'translation'. Maximum growth is reached at terminal time, before the resulting unblended spirals are stirred back into trailing spirals. Though the whole process is clearly inviscid, viscosity plays a rôle in

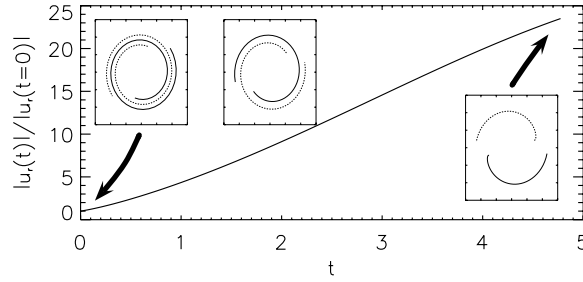


FIG. 5: Illustration of the initial destructive interference of vorticity spirals.

the selection of the initial characteristic radial scale of the optimal disturbance (the greater the Reynolds number, the thinner the vorticity sheets).

We now present a simple model intended to mimic the combined effects of advection and induction, and to illustrate the initial destructive interference between vorticity spirals. In this model, the evolution of points vortices advected by an $1/r$ flow initially organized along spirals is examined, and the resulting induced velocity at the center is evaluated. Starting with two filaments rolled up in spiral form, the action of the mean external shear flow ($\simeq 1/r$) is to materially advect the vorticity and to concentrate the spiral. Figure 5 represents the evolution of resulting radial velocity at the center, which is a measure of the induction term. Its action is negligible at initial time, due to destructive interference of intertwined spirals. But, as time evolves, the spirals become unwound. As a consequence, their action focuses on the centre and redirects vorticity from the mean flow to the perturbation.

The important point of the present letter is that $m = 1$ disturbances injected in a vortex are subject to transient amplification. The physical mechanism feeding the transient growth is not restricted to a local Orr mechanism, but includes also a global effect of vortex induction. It is noteworthy that these two mechanisms are not specific to the Lamb-Oseen vortex, or even to vortices, but are generic to free flows with the two hydrodynamic ingredients: shear and rotation. Nevertheless, several questions remain unanswered. First, in the linear regime, what are the respective roles of stretching and tilting in the 3D case? Is the

peak in figure 1 the result of a resonance phenomenon? Moreover, the nonlinear regime of the optimal perturbation will be investigated via direct numerical simulations in order to address the relevance of a ‘by-pass’¹⁴ transition scenario in such a flow. Back to aircraft vortices, the similarity between the result of optimal evolution (a core contamination by external disturbance leading to a translation) and the long-wave erratic displacements of experimental vortices, a phenomenon known as *vortex meandering*²³, also encountered in tornado- and hurricane-like flows¹¹, appears puzzling and worthy of further investigation. Finally, an exhaustive parametric study is currently under way in order to investigate other azimuthal wavenumbers and the influence of base flow diffusion²⁵.

-
- ¹ S. C. Crow. Stability theory for a pair of trailing vortices. *AIAA J.*, 8(12):2172–2179, 1970.
 - ² T. Leweke and C. H. K. Williamson. Cooperative elliptic instability of a vortex pair. *J. Fluid Mech.*, 360:85–119, 1998.
 - ³ E. W. Mayer and K. G. Powell. Viscous and inviscid instabilities of a trailing line vortex. *J. Fluid Mech.*, 245:91–114, 1992.
 - ⁴ D. Fabre. *Instabilités et instationnarités dans les tourbillons : application aux sillages d’avions*. PhD thesis, Université Paris VI, 2002.
 - ⁵ R. J. Briggs, J. D. Daugherty, and R. H. Levy. Role of landau damping in cross-field electron beams and inviscid shear flow. *Phys. Fluids*, 13:421–432, 1970.
 - ⁶ D. A. Schecter, D. H. E. Dubin, A. C. Cass, C. F. Driscoll, I. M. Lansky, and T. M. O’Neill. Inviscid damping of asymmetries on a two-dimensional vortex. *Phys. Fluids*, 12(10):2397–2412, 2000.
 - ⁷ A.J. Bernoff and J.F. Lingeitch. Rapid relaxation of an axisymmetric vortex. *Phys. Fluids*, 6:

- 3717–3723, 1994.
- ⁸ K. Bajer, A. P. Bassom, and A. D. Gilbert. Accelerated diffusion in the centre of a vortex. *J. Fluid Mech.*, 437:395–411, 2001.
 - ⁹ R. A. Smith and M. N. Rosenbluth. Algebraic instability of hollow electron columns and cylindrical vortices. *Phys. Rev. Lett.*, 64(6):649–652, 1990.
 - ¹⁰ D. S. Nolan and M. T. Montgomery. The algebraic growth of wavenumber one disturbances in hurricane-like vortices. *J. Atmos. Sci.*, 57:3514–3538, 2000.
 - ¹¹ D. S. Nolan and B. F. Farrell. Generalized stability analyses of asymmetric disturbances in one- and two-celled vortices maintained by radial inflow. *J. Atmos. Sci.*, 56:1282–1307, 1999.
 - ¹² D. S. Nolan and B. F. Farrell. The intensification of two-dimensional swirling flows by stochastic asymmetric forcing. *J. Atmos. Sci.*, 56(23):3937–3962, 1999.
 - ¹³ T. Miyazaki and J.C.R. Hunt. Linear and nonlinear interactions between a columnar vortex and external turbulence. *J. Fluid Mech.*, 402:349–378, 2000.
 - ¹⁴ L. N. Trefethen, A. E. Trefethen, S. C. Reddy, and T. A. Driscoll. Hydrodynamic stability without eigenvalues. *Science*, 261:578–584, July 1993.
 - ¹⁵ K. M. Butler and B. F. Farrell. Three-dimensional optimal perturbations in viscous shear flow. *Phys. Fluids*, 4:1637–1650, 1992.
 - ¹⁶ D. G. Lasseigne, R. D. Joslin, T. L. Jackson, and W. O. Criminale. The transient period for boundary layer disturbances. *J. Fluid Mech.*, 381:89–119, 1999.
 - ¹⁷ P. Luchini and A. Bottaro. Görtler vortices : a backward-in-time approach to the receptivity problem. *J. Fluid Mech.*, 363:1–23, 1998.
 - ¹⁸ P. Luchini. Reynolds-number-independant instability of the boundary layer over a flat surface : optimal perturbations. *J. Fluid Mech.*, 404:289–309, 2000.

- ¹⁹ P. Corbett and A. Bottaro. Optimal linear growth in swept boudary layers. *J. Fluid Mech.*, 435:1–23, 2001.
- ²⁰ B. Fornberg. *A Practical Guide to Pseudospectral Methods*. Cambridge University Press, 1995.
- ²¹ J. A. C. Weideman and S. C. Reddy. A MATLAB differentiation matrix suite. *ACM Trans. Math. Soft.*, 26(4), 2000.
- ²² B. F. Farrell and P. J. Ioannou. Optimal excitation of three-dimensional perturbations in viscous constant shear flow. *Phys. Fluids*, 5(6):1390–1400, 1993.
- ²³ L. Jacquin, D. Fabre, P. Geffroy, and E. Coustols. The properties of a transport aircraft wake in the extended near field : an experimental study. *AIAA P.*, 2001-1038, 2001.
- ²⁴ at least within the numerical limits.
- ²⁵ Preliminary results reveal that this influence is marginal, at least for the range of Reynolds numbers considered here.

Figure 1 Optimal energy growth and corresponding optimal time (in rotation periods) versus axial wavenumber.

Figure 2 Isosurfaces of axial vorticity for the optimal 3D case. The levels correspond to ± 80 % of maximum vorticity, at initial time (left) and optimal time (right).

Figure 3 Evolution of growth with terminal time (in rotation periods) in the 2D case at $\text{Re} = 1000$.

Figure 4 Cross section of axial vorticity in the 2D case. The contour plot levels are ± 60 % of maximum absolute vorticity.

Figure 5 Illustration of the initial destructive interference of vorticity spirals.

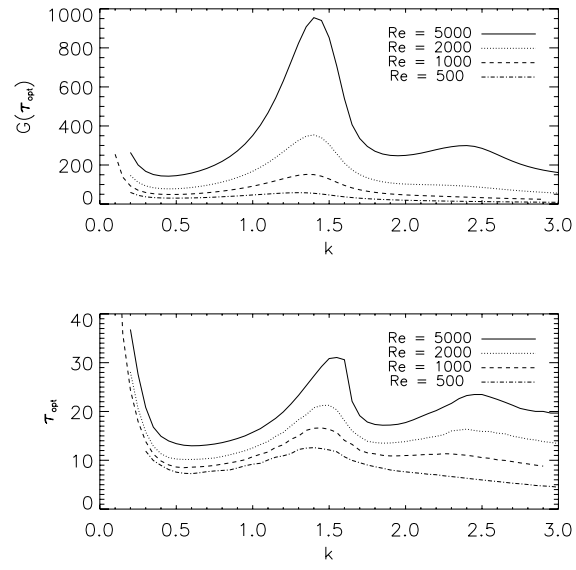


Figure 1, Antkowiak, Physics of Fluids.

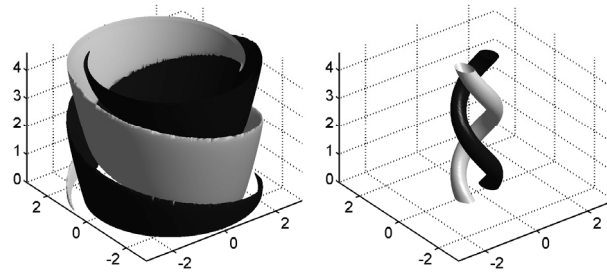


Figure 2, Antkowiak, Physics of Fluids.

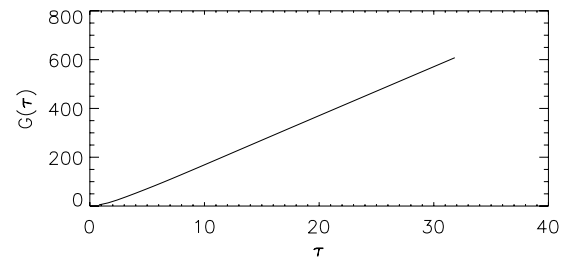


Figure 3, Antkowiak, Physics of Fluids

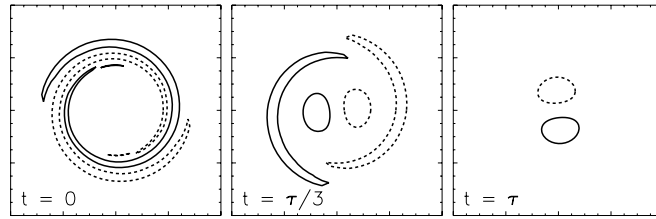


Figure 4, Antkowiak, Physics of Fluids

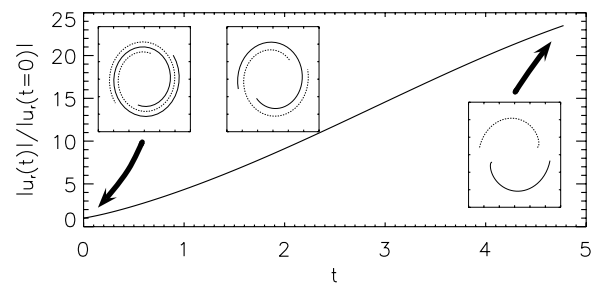


Figure 5, Antkowiak, Physics of Fluids